PHYSICAL REVIEW E **76**, 050402(R) (2007)

Construction and stability of a close-packed structure observed in thin colloidal crystals

Ana Barreira Fontecha, Thomas Palberg, and Hans Joachim Schöpe*
Institut für Physik, Johannes Gutenberg–Universität Mainz, Staudingerweg 7, D-55128 Mainz, Germany
(Received 26 July 2007; published 6 November 2007)

We have characterized a close-packed structure of confined charged colloidal spheres, which has been recently discovered. Using different microscopy experiments, the vertically arranged hexagonal planes of n-hcp$\perp$ are found to continuously evolve from the horizontally oriented stacks of n hexagonal planes ($n\Delta$) following the maximum packing criterion, but discontinuously transform to a stack of $n+1$ square planes [$(n+1)\square$]. Large mechanically stable domains with threefold twin structures are regularly observed in the suspended state at packing fractions between 0.4 and 0.58.

DOI: 10.1103/PhysRevE.76.050402 PACS number(s): 82.70.Dd, 61.72.Nn, 64.70.Dv

The packing of spheres in confined geometry is of both fundamental and practical interest for logistics, mathematics, condensed matter physics, and recently also in colloid science [1–3]. For colloids in the bulk, body centered cubic (bcc) packing is observed at long ranged repulsions, while face centered cubic (fcc), hexagonal close packing (hcp), and randomly stacked hexagonal planes (r-hcp) are thermodynamically stable for short ranged interactions including the theoretical limit of hard spheres. The latter reach a maximum packing fraction of $\Phi=0.74$. Restricting the available space leads to adaptations of these structures to the symmetry of the confinement and a rich variety is found as a function of colloid packing fraction and confinement dimension. Their practical importance lies within their use as (precursors of) photonic and phononic materials [4,5], while at the same time there is a fundamental interest in understanding this diversity in terms of thermodynamics, kinetics, and the influence of external forces.

Seminal work confining colloidal crystals between two plates showed a sequence of transitions with increasing plate to plate distance H: $1\triangle \Rightarrow 2\square \Rightarrow 2\triangle \Rightarrow 3\square \Rightarrow \cdots \Rightarrow n\triangle \Rightarrow (n+1)\square \Rightarrow \cdots$. Here n denotes the layer number and $\triangle$ and $\square$ denote triangular or square symmetry, respectively. To be specific, Pieranski *et al.* [3,6] used a wedge geometry to observe several structures in parallel, an approach followed also in almost all later work. Both packings derive from placing the fcc-(111) and fcc-(100) faces of the close-packed structures parallel to the confining walls. For three and more layers, *ABA* (hcp) or *ABC* (fcc) stacking or irregular stacking sequences (r-hcp) are possible. For particle sizes larger than ~300 nm, this results in fascinating color effects allowing fast tracing of sequences on a macroscopic scale [Fig. 1(a)] [7].

Further crystalline structures were observed mediating between $n\square$ and $n\triangle$ as well as between $n\triangle$ and $(n+1)\square$. In particular, a buckling phase B in the $1\triangle \Rightarrow 2\square$ transition, a rhombohedric phase R in the $2\square \Rightarrow 2\triangle$ transition, and prism phases P mediating for the $n\triangle \Rightarrow (n+1)\square$ transition were discovered in cells with minimized solvent evaporation and salt gradients [8–10]. Here, mechanical forces due to solvent flow or surface tension were reduced and large domain sizes realized using very small wedge angles. On the theoretical side now the "full equilibrium phase diagram" of confined hard spheres is available as well as extensions for charged and even attractive spheres [11–14].

Recently, another structure was reported, occurring in $n\triangle \Rightarrow (n+1)\square$, which we will call in the following n-hcp$\perp$ [7,15]. Like $n\triangle$ and $n\square$, it derives from a close-packed structure (hcp) but is vertically oriented with the hcp-(210) face parallel to the confining walls. While observed in experiments, it is not predicted in theoretical ground state calculations for hard spheres [14]. Our Rapid Communication therefore addresses the construction principles and structural properties of n-hcp$\perp$ under different experimental conditions, aiming to contribute to both the fundamental question of stability and the practical issue of fabrication.

We compare suspended and dried structures using high-resolution microscopy, small aperture microscopy, and low-order Bragg scattering (Fourier microscopy [7,16]) on suspended structures as well as scanning electron microscopy for dry samples. Charged stabilized colloidal spheres of different diameters ($0.5<\sigma<1.2$ μm) with polydispersities between 1.2% and 3% were used in our experiments. Particles were suspended in carbonate-saturated ultrapure water ($c=5.6$ μmol l^{-1}) to avoid salt gradients. We used different cells with wedge angles of 1 mrad and less to maximize the domain size. One group of cells were glued in a watertight fashion between two microscopy slides (70×20 mm^2) with a 50 μm spacer included at one side. Some were fully sealed, some were connected at the wide side to a bulk reservoir of particles, and some were left open at the narrow side to allow ultraslow evaporation into a constant 90% humidity atmosphere, yielding drying times of up to several weeks. For the other group of cells we used Pieranski's setup. Here a spherical glass top plate is placed in contact with a glass slide which is glued at the bottom of a stainless-steel cylinder. A Viton ring between the spherical cap and the border of the reservoir assures the correct sealing. For all these cells, significant salt concentration gradients, solvent currents, and capillary forces were absent.

Still, the particles are observed to migrate slowly (within a few days) to the narrow side of the cell and assemble into different crystal structures at growth rates of about 1 μm/h. Independent of the initial concentration, the final (wet state) concentrations always were found in the range of $0.4\leq\Phi$

*jschoepe@uni-mainz.de

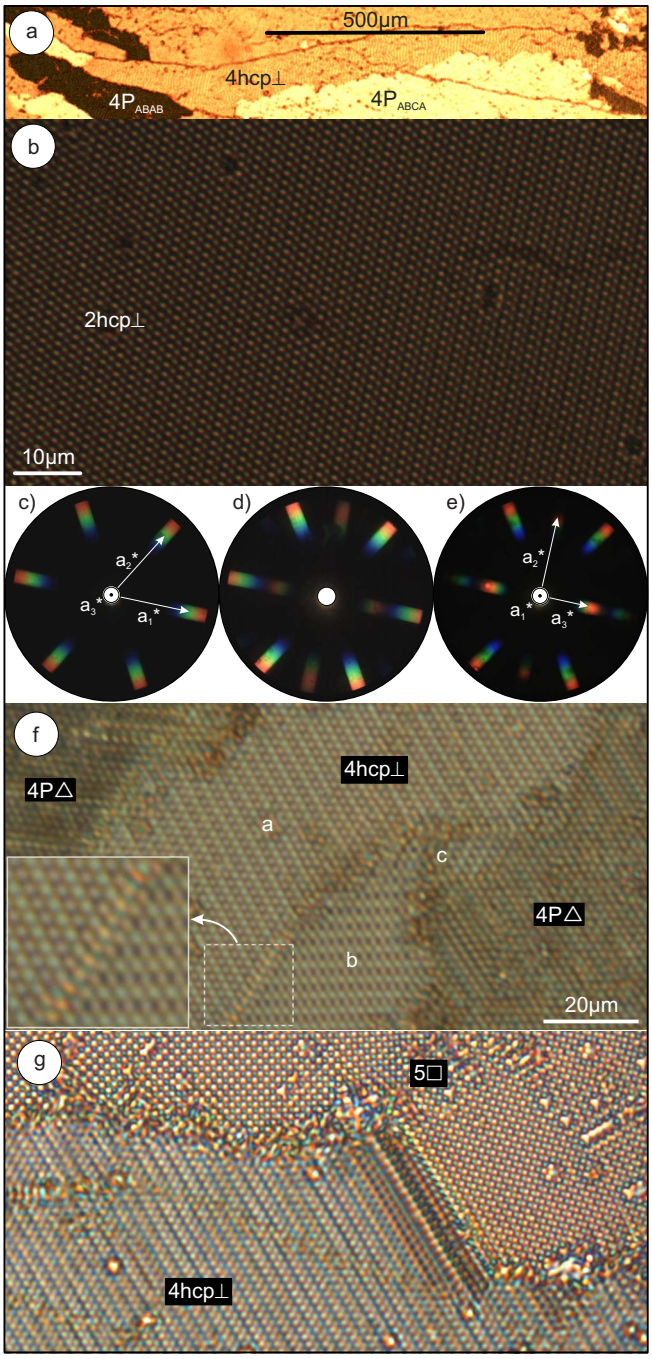

FIG. 1. (Color online) Optical micrographs of n-hcp⊥. (a) Overview from small aperture microscopy. Note shape and size of domains and coexistence with other intermediates. (b) n-hcp⊥ for $n=2$. (c)–(e) Fourier micrographs of the 2△ to 2-hcp⊥ transition showing a continuous transformation; (c) hcp (001), (d) intermediate structure, (e) hcp(210). a_1^*, a_2^*, and a_3^* are reciprocal lattice vectors. (f) Coexistence of 4-hcp⊥ with $4P$△. Note the twin formation of hcp⊥ (areas a, b, c). The inset shows a twin boundary in detail. (g) Abrupt transformation of 4-hcp⊥ to 5□. Note the possible retention of orientation in the transition to $(n+1)$□.

≤0.58 as expected for charged spheres. Upon drying, the originally assembled structures were compressed under the influence of capillary forces to optimize packing. It is observed that some of the existing structures in the wet state

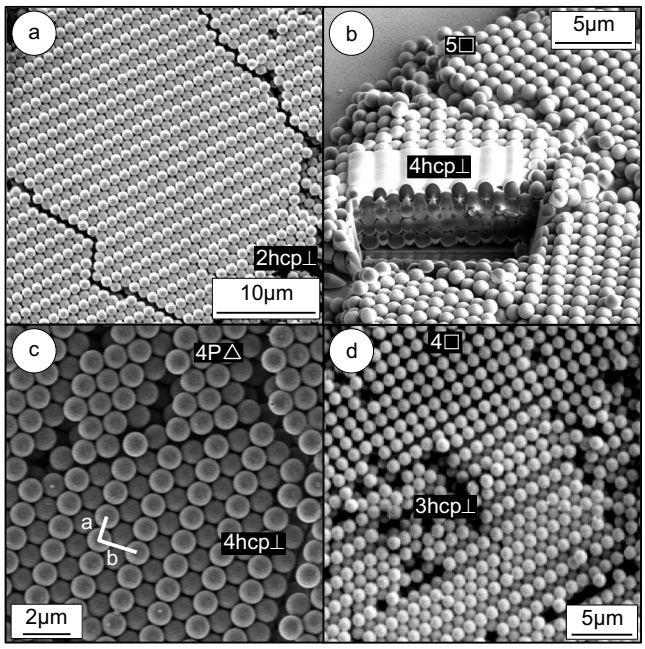

FIG. 2. Electron micrographs of dried samples. (a) n-hcp⊥ for $n=2$. (b) Cut through 4-hcp⊥. Coexistence with 5□. (c) Coexistence of 4-hcp⊥ with $4P$△. Note the sharp domain boundary in the dry sample. (d) Abrupt transformation of 4-hcp⊥ to 5□. As in (c) the crystal orientation is maintained.

(thermodynamic equilibrium) are destroyed during drying while others are not. In the following we will call the latter mechanically stable structures because they withstand lateral compression.

Several micrographs in Figs. 1 and 2 show the structure and morphology of n-hcp⊥, the coexistence with other intermediate structures, and its transition from n△ to $(n+1)$□. In the wet state, the n△ ⇒ $(n+1)$□ transition is observed for n values up to 7. Figure 1(a) shows part of the 4△ ⇒ 5□ transition. We observe large domains of 4hcp⊥ up to 1000×200 μm^2 extended in the growth direction. High-resolution microscopy reveals a high structural quality of the n-hcp⊥ domains [Figs. 1(b) and 2(a)]. In top view parallel rows of elevated particles are separated by lower-lying rows. On first view this structure recalls the buckling phase in the 1△ to 2□ transition. To assess the structure of the hidden layers, we sputtered the surface of a selected region with Pt and subsequently cut a rectangular box using Ga-ion beam etching. The cut through the crystal in Fig. 2(b) nicely shows the vertically oriented hexagonal layers. Due to its orientation, n-hcp⊥ shows hexagonal domain shape [Fig. 1(f)] which facilitates the formation of twin structures [regions marked a–c in Fig. 1(f)] with three possible orientations connected by domain boundaries of very small width, either one or even zero "buffer layer" [inset of Fig. 1(f)]. Like P and B, but unlike other intermediates, n-hcp⊥ is mechanically stable upon drying, irrespective of orientation. Different structures coexists with n-hcp⊥. There is a coexistence with other structures like nP△ and $(n+1)$□, and no smooth transition between these structures can be observed in either the suspended [Figs. 1(f) and 1(g)] or the dry state [Figs. 2(b)–2(d)]. There is also a possible retention of orientation

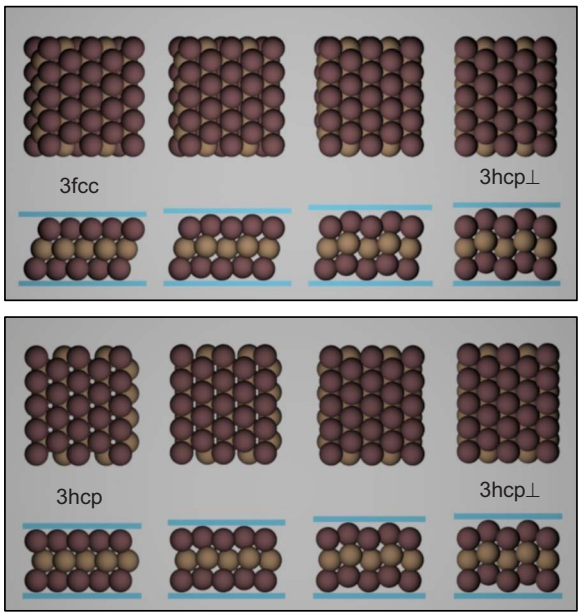

FIG. 3. (Color online) Model for the transition $n\triangle$ to n-hcp$\perp$ in top and side views. Top, the transition $n\triangle$ (fcc) to n-hcp$\perp$. Bottom, the transition $n\triangle$ (hcp) to n-hcp$\perp$. For details, see text.

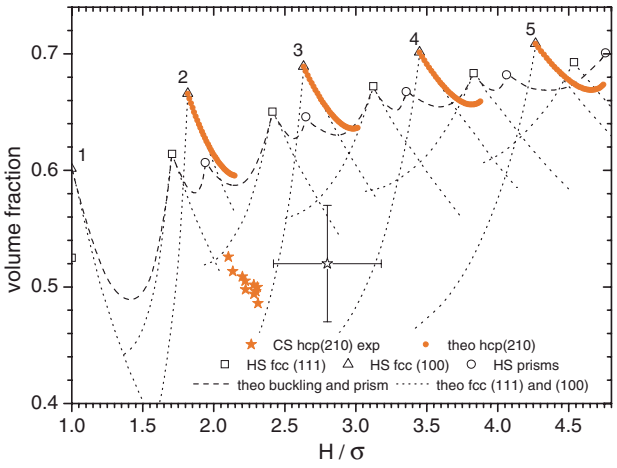

FIG. 4. (Color online) Crystal volume fraction vs normalized cell height. The red filled stars show the experimental data for 2-hcp$\perp$. The error bar represents the systematic error. The red filled circles show the packing fraction behavior for the hcp$\perp$ transition for hard spheres. The open symbols indicate the stable hard sphere structures. The dotted lines show the behavior of Φ when a structure does not match the wedge height [6]. The dashed line shows the buckling transition and the transition between $\square$ and $P\triangle$ [9].

observable for the transition to $(n+1)\square$ [Figs. 1(g) and 2(d)].

Upon increasing the cell height H, $n\triangle$ smoothly converts to n-hcp$\perp$. The ratio of distances b between rows to in-row distances $a=\sigma+x$ [Fig. 2(c); x is the surface separation of the spheres] is taken either directly from calibrated micrographs or from the scattering patterns, which show a continuous transition from $n\triangle$ to n-hcp$\perp$ [Figs. 1(c)–1(e)] with increasing cell height H. Figure 1(c) shows the hexagonal scattering pattern of the $2\triangle$ structure. The reciprocal lattice vectors a_1^*, a_2^*, and a_3^* are drawn for clarity. The scattering pattern of the 2-hcp$\perp$ is represented by Fig. 1(e). As the pattern is generated by only two layers and so the reciprocal lattice consists of Bragg rods, the pattern shows the in-plane periodicity of a single layer, which is different from the scattering pattern obtained from a bulk crystal. For thin layers the $(h,1,0)$ and $(h,0,1)$ reflections are visible, while they are forbidden for a higher number of layers. Across the transition, a small continuous distortion of the hcp unit cell takes place: e.g., close to $2\triangle$ $b/a\approx 1.7\pm 0.01$ while close to $3\square$ $b/a\approx 1.62\pm 0.01$. Assuming a particle surface–cell wall distance $d\approx x$, the packing fractions decrease slightly from $\Phi\approx 0.53$ to $\Phi\approx 0.49$ in the suspended state. This differs considerably from the ideal hcp, touching hard sphere values of $b/a=1.633$ and $\Phi_{\mathrm{HS}}=0.6535$ for $n=2$. In the dry state, $b/a=1.65\pm 0.01$ is close to the ideal value [Figs. 2(a)–2(d)].

Since in the $n\triangle$ to n-hcp$\perp$ transformation a rotation of the constituting elements also occurs, the mechanism is more complicated than for buckling or prism formation, which only involves uniaxial compression and shift of elements. Depending on the stacking sequence of $n\triangle$ (hcp or fcc) two possible transitions to n-hcp$\perp$ are possible following the maximum packing criterion (Fig. 3). The transformation of $n\triangle$ (fcc) ([111] $\perp$ to the substrate) to n-hcp$\perp$ can be described by an upward rotation of $(\bar{1}\,\bar{1}1)$ planes around the $[1\bar{1}0]$ axis and slightly shifting every second $(\bar{1}\,\bar{1}1)$ plane with respect to each other along their grooves ($\langle\bar{1}\,\bar{1}2\rangle$ direction) into the local energy minimum. The transformation of $n\triangle$ (hcp) stacking ([001] $\perp$ to the substrate) to n-hcp$\perp$ can be described by sliding every second (001) plane in the [210] direction and by shifting every second row ($\|$[010] axis) of the (001) planes in the [001] direction following the maximum packing criterion.

Figure 4 shows the crystal volume fraction for several structures as function of the normalized cell height. For the ideal hard sphere case, starting from $n\triangle$, b/a continuously decreases, while Φ_{HS} shows a shallow minimum. Experimentally, the former is confirmed for $3\triangle\Rightarrow$3-hcp$\perp$, while the latter is masked by experimental error. In the transition region from $\triangle$ to $\square$, hcp$\perp$ is more stable using the maximum packing criterion than P, $\triangle$, and $\square$. Therefore it is surprising that n-hcp$\perp$ is not found in ground state calculations for confined hard spheres [14].

Experimentally, however, n-hcp$\perp$ is observed to coexist in the suspended and in the dried state with $nP\triangle$, $nP\square$, $(n+1)\square$, and a number of other intermediates of more irregular structure [7,15]. For all suspended structures we found $\Phi<\Phi_{\mathrm{HS}}$. This seems to indicate an energetic degeneracy of all these structures at finite temperature, possibly supported by the presence of the soft electrostatic repulsion. Alternatively, there may be a kinetic bias circumventing thermodynamics, since, once a structure is formed by local fluctuations (nucleated), further particles will arrange epitaxially according to their template until the next phase nucleates.

We have shown that n-hcp$\perp$ may be formed at comparably low Φ from charged spheres. It is mechanically stable and survives compression by capillary forces. In the ideal hard sphere case n-hcp$\perp$ follows the maximum packing criterion. It is formed by a smooth transition from $n\triangle$ but no

smooth transition to $(n+1)\square$ is observed. These observations may have significant implications for the fabrication of useful mechanically stable structures on a larger scale, but also stimulate further theoretical and experimental efforts devoted to the structural properties of confined colloids.

We thank H. Löwen and R. Goldberg for fruitful discussions and M. Kappl for doing some of the SEM measurements, and acknowledge financial support of DFG (SFB TR6), EU (Grant No. MRTN-CT-2003-504712), Forschungsfond, and MWFZ, Mainz.

[1] J. D. Bernal and J. Mason, Nature (London) **188**, 910 (1960).
[2] S. E. Phan, W. B. Russel, J. Zhu, and P. M. Chaikin, J. Chem. Phys. **108**, 9789 (1998).
[3] P. Pieranski, L. Strzelecki, and B. Pansu, Phys. Rev. Lett. **50**, 900 (1983).
[4] F. Meseguer, Colloids Surf., A **270**, 1 (2005).
[5] W. Cheng, J. Wang, U. Jonas, G. Fytas, and N. Stefanous, Nat. Mater. **5**, 830 (2006).
[6] B. Pansu, Pi. Pieranski, and Pa. Pieranski, J. Phys. (Paris) **45**, 331 (1984).
[7] H. J. Schöpe, A. Barreira Fontecha, H. König, J. Marques Hueso, and R. Biehl, Langmuir **22**, 1828 (2006).
[8] S. Neser, P. Leiderer, and T. Palberg, Prog. Colloid Polym. Sci. **102**, 194 (1997).
[9] S. Neser, C. Bechinger, P. Leiderer, and T. Palberg, Phys. Rev. Lett. **79**, 2348 (1997).
[10] A. Barreira Fontecha, H. J. Schöpe, H. König, T. Palberg, R. Messina, and H. Löwen, J. Phys.: Condens. Matter **17**, S2779 (2005).
[11] M. Schmidt and H. Löwen, Phys. Rev. E **55**, 7228 (1997).
[12] R. Zangi and S. A. Rice, Phys. Rev. E **61**, 660 (2000); **61**, 671 (2000).
[13] R. Messina and H. Löwen, Phys. Rev. Lett. **91**, 146101 (2003).
[14] A. Fortini and M. Dijkstra, J. Phys.: Condens. Matter **18**, L371 (2006).
[15] F. Ramiro-Manzano, F. Meseguer, E. Bonet, and I. Rodriguez, Phys. Rev. Lett. **97**, 028304 (2006).
[16] R. Biehl and T. Palberg, Rev. Sci. Instrum. **75**, 906 (2004).